Eur. J. Mech., A/Solids, **12**, n° 4, 445-470, 1993

Preisach model and hysteretic behaviour of ductile materials

V. A. LUBARDA *, D. SUMARAC ** and D. KRAJCINOVIC *

ABSTRACT. – This paper presents an application of the Preisach model of hysteresis to analysis of the hysteretic response of ductile materials subjected to cyclic loading or straining. The proposed method is applied to various material models, obtained by series or parallel connections of elastic and plastic elements. Energy dissipation and the locked-in energy are determined for the primary loading and any subsequent unloading and reloading. Finally, the paper presents a discussion of the hardening characteristics and anisotropic response.

1. Introduction

The phenomenon of hysteresis, which occurs in various branches of physics, has been a long-standing topic of research interest. Its description by what is today known as Preisach model goes back to an early paper by [Preisach, 1935], which deals with the magnetization hysteresis. Later development occured in describing other hysteretic phenomena, such as adsorbtion hysteresis [Everett & Whitton, 1952]. However, despite its powerfull mathematical structure and many advantages, this method has as yet to be applied to problems of solid mechanics. This paper focuses on the application of the Preisach model to the description of the hysteretic response of ductile materials subjected to cyclic stress or strain.

To emphasize the mathematical structure of the Preisach model and to analize the hysteretic behaviour, various series and parallel connections of elastic (spring) and plastic (slip) elements are considered, similar to original [Masing, 1926] parallel-bar model. Some of these material models were used by [Iwan, 1967] in his analysis of the anisotropic yielding behaviour, and more recently by [Conle *et al.*, 1988] in their analysis of the fatigue behaviour. In this paper precise evaluation of the energy dissipation is done, including distinction between energy dissipated into heat and the locked-in energy. The locked-in energy is calculated for each cycle and correlated to the hardening characteristics and anisotropic response during unloading from the plastic state and reverse loading and reloading. Considered model also leads to an unambiguous identification of material parameters from the experimental data.

* Mechanical and Aerospace Engineering, Arizona State University, Tempe, AZ 85287-6106, USA.
** Civil Engineering, University of Belgrade, Belgrade, Yugoslavia.

EUROPEAN JOURNAL OF MECHANICS, A/SOLIDS, VOL. 12, N° 4, 1993
0997-7538/93/04 445 26/$ 4.00/

The rigorous mathematical structure of the proposed model allows for a variety of extensions and modifications to a host of related, experimentally observed phenomena, such as cyclic hardening or softening to a stable cycle, cyclic creep and relaxation, etc. ([Mroz *et al.*, 1975]; [Drucker & Palgen, 1981]; [Chaboche, 1986]; [Bower, 1989]; [Suresh, 1991]). Further extensions to ductile-brittle behaviour including successive failure of individual elements and a resulting cascade mode of the failure ([Krajcinovic & Silva, 1982]; [Hult & Travnicek, 1983]; [Mroz, 1983]) are possible as well, and will be a subject of the subsequent paper.

2. The Preisach model of hysteresis

An outline of the Preisach model of hysteresis behavior, utilized in this paper, is presented in this section. For a more detailed and comprehensive analysis, the recent monograph by [Mayergoyz, 1991] should be consulted. The phenomenon of hysteresis, which occurs in various branches of physics (mechanics, magnetism and optics, for example), has been a topic of long-standing research interest. Nonlinear behaviour associated with the hysteresis (hysteresis nonlinearity) can be of local and/or nonlocal memory. In the first case, the value of the output function $f(t)$ (say, stress) at time $t \geqq t_0$ is uniquely determined by the input (strain) values $u(t)$ at $t \geqq t_0$ and by the output (stress) value $f(t_0)$. History influences the future behaviour only through the current value of the output function. If the hysteresis possesses nonlocal memory, the future values of output also depend on the past extremum values of input and corresponding outputs. Both of these nonlinearities can be represented the Preisach model of hysteresis. Nonlinearities of both types can be modeled by the superposition of elementary hysteresis operators having local memory.

The Preisach model implies mapping of input $u(t)$ on output $f(t)$ in the form of an integral

$$f(t) = \iint_{\alpha \geqq \beta} \mathrm{P}(\alpha, \beta)\, \mathrm{G}_{\alpha,\beta}\, u(t)\, d\alpha\, d\beta. \tag{1}$$

In (1) $\mathrm{G}_{\alpha,\beta}$ is an elementary hysteresis operator representing geometrically a rectangular loop shown in Figure 1. Parameters α and β are up and down switching values of the input, and $+1$ and -1 are two possible output values. As the input $u(t)$ is monotonically increased, the ascending branch *abcde* is followed; when decreased, the descending branch *edfba* is traced. $\mathrm{P}(\alpha, \beta)$ is the Preisach function, a weight function of the hysteresis nonlinearity to be represented by the Preisach model. On physical ground it is natural to assume that $\alpha \geqq \beta$. Thus, the integration in (1) is performed over the right triangle in (α, β) plane, with line $\alpha = \beta$ being the hypotenuse and point $(\alpha_0, \beta_0 = -\alpha_0)$ being the triangular vertex. The value of $\alpha_0 > 0$ is defined by the largest extremum value of the input function $u(t)$. Each point within this triangle corresponds to a particular $\mathrm{G}_{\alpha,\beta}$ operator, with switching values equal to (α, β) coordinates of that point. The triangle

(*Fig.* 2) is called a limiting triangle providing support for the Preisach function, since the Preisach function $P(\alpha, \beta)$ is assumed to vanish outside the triangle.

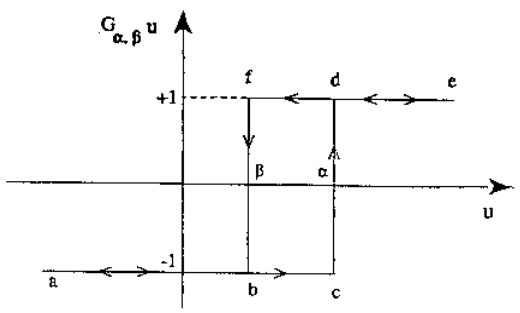

Fig. 1

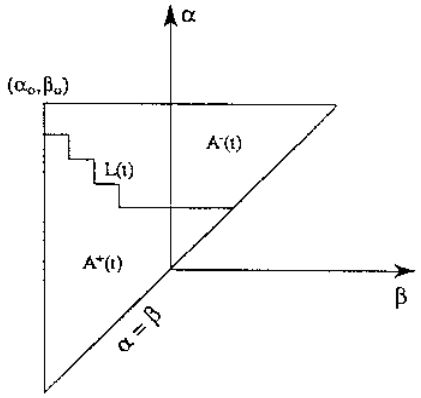

Fig. 2

Fig. 1. – Elementary hysteresis operator represented by a rectangular loop. α and β are the up and down switching values of the input, and +1 and −1 are the two possible output values.
Fig. 2. – Limiting triangle with a staircase interface line $L(t)$ separating two parts $A^-(t)$ and $A^-(t)$, with +1 and −1 output values of the elementary hysteresis operator.

For example, if the input u initially has the value less than β_0, the outputs of all $G_{\alpha,\beta}$ operators within a triangle are equal to −1 (a state of negative saturation). If the input is then monotonically increased to value u_1, all $G_{\alpha,\beta}$ operators with up switching value $\alpha < u_1$ have outputs changed to +1. If the input is subsequently decreased to value u_2, all $G_{\alpha,\beta}$ operators with down switching values $\beta > u_2$ are turned back to output value −1. The subdivision of the triangle, defining positive and negative outputs of $G_{\alpha,\beta}$ operators, proceeds in an obvious manner, corresponding to any particular history of the input variation $u(t)$. The interface between two parts of the triangle is a staircase line $L(t)$ (*Fig.* 2), whose vertices have (α, β) coordinates that are local input maxima and minima at previous instants of time. If the input is momentarily being increased, the final link of $L(t)$ is horizontal, if it is decreased, it is vertical. Therefore, if $A^+(t)$ and $A^-(t)$ denote two parts of the limiting triangle, separated by line $L(t)$, the Preisach formula (1) becomes

$$f(t) = \iint_{A^+(t)} P(\alpha, \beta)\, d\alpha\, d\beta - \iint_{A^-(t)} P(\alpha, \beta)\, d\alpha\, d\beta. \tag{2}$$

A given hysteresis nonlinearity can be represented by the Preisach model if it possesses the so-called wiping out and congruency properties. Indeed, from Figure 2 it is clear that each local input maximum wipes out the vertices of the interface $L(t)$ whose α coordinates are below this maximum, and similarly each local minimum wipes out the vertices whose β coordinates are above this minimum. In other words, only the alternating series of dominant input extrema are stored by the Preisach model, while the other

extrema are wiped out (*Fig.* 3). Of course, the subsequent events may erase previously stored informations, if the new input extrema are larger than the previous ones.

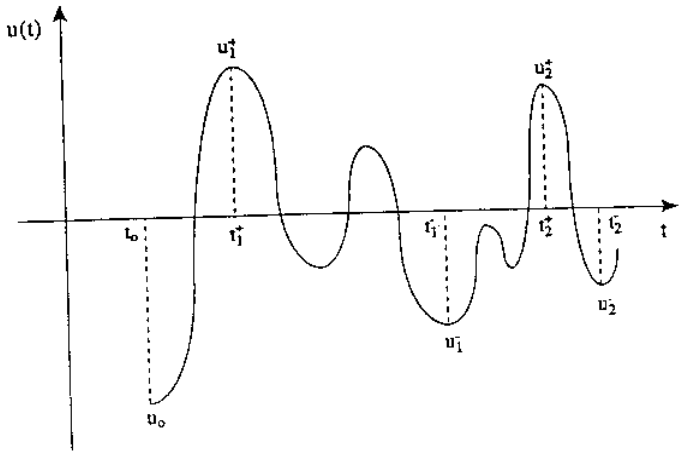

Fig. 3. Preisach model stores only alternating series of dominant input extrema (u_1^+, u_1^-, u_2^+, u_2^-,...). All others extrema are wiped out.

The congruency property of the Preisach model is related to periodic input variations. All minor hysteresis loops corresponding to back-and-forth variation of input between the same two consecutive extremum values are congruent. Such minor loops, obtained by reversal from ascending or descending branch of the major loop, can only be shifted relatively to each other along the output axes (*Fig.* 4).

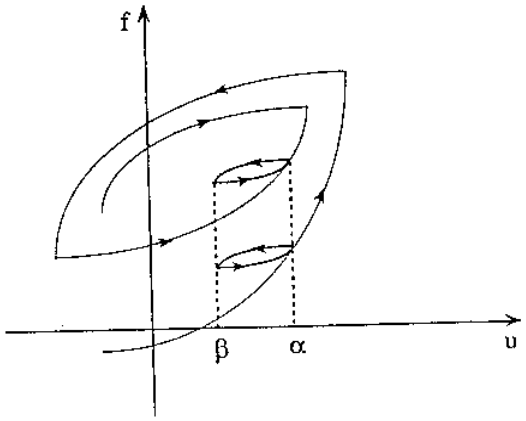

Fig. 4

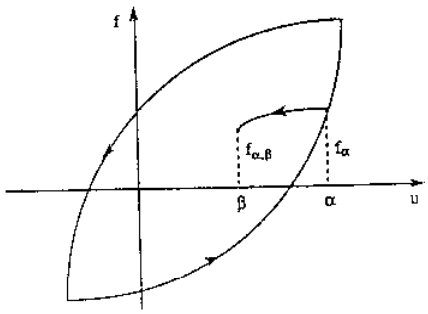

Fig. 5

Fig. 4. – Congruency property of the Preisach model. Minor loops corresponding to back-and-forth variation of input between the same two extremum values are congruent.

Fig. 5. – First-order transition curve obtained by input reversal from $u=\alpha$ to $u=\beta$. f_α is the output value at $u=\alpha$ corresponding to the ascending branch of the major loop, while $f_{\alpha,\beta}$ is the output value at $u=\beta$ along the transition curve.

For a given hysteresis nonlinearity, the Preisach weight function $P(\alpha, \beta)$ can be determined as follows. Starting from the state of negative saturation, let the input be increased to some value α. The output follows ascending branch of the major loop, and at input $u=\alpha$ has the value f_α. If the input is subsequently decreased to some value β, the output follows the corresponding reversal (transition) curve, as sketched in Figure 5. Denoting the output value at $u=\beta$ by $f_{\alpha,\beta}$, it then follows from the limiting triangle

$$f_{\alpha,\beta} - f_\alpha = 2\int_\beta^\alpha \left[\int_{\beta'}^{\alpha} P(\alpha', \beta')\, d\alpha'\right] d\beta', \tag{3}$$

where from by differentiation with respect to β and α, respectively, one finds

$$P(\alpha, \beta) = \frac{1}{2}\frac{\partial^2 f_{\alpha,\beta}}{\partial\alpha\,\partial\beta}. \tag{4}$$

An analogous expression is obtained when the reversal curve is attached to the descending branch of the major loop (an increasing transition curve). Also, it is easy to show that $P(\alpha, \beta)$ possesses a mirror symmetry with respect to line $\alpha+\beta=0$, *i.e.* $P(-\beta, -\alpha)=P(\alpha, \beta)$. If the hysteresis nonlinearity satisfies the wiping-out and congruency properties, the Preisach function $P(\alpha, \beta)$ is the same regardless of which transition curves are used to determine it. From a practical point of view, the most advantageous approach is to use the so-called first-order transition curves, obtained by the first reversal from either ascending or descending branches of the major loop, since they are in experimental observation of the hysteresis easier to detect.

If the hysteresis nonlinearity does not exactly satisfies the wiping-out and congruency properties, the weight function $P(\alpha, \beta)$ determined from different transition curves is in general different, and the Preisach model is inappropriate. One can, however, try to predict or accurately guess a possible regimes in which the model will be used, and consequently determine $P(\alpha, \beta)$ by matching the transition curves from that region. It is also noted that the determination of the weight function from formula (4) implies differentiation from experimentally determined values. Since this can largely increase the errors present in any experimental data, differentiation is usually replaced by an adequate numerical procedure which completely circumvents the difficulty. This is in detail discussed in [M, 1991], and for the economy in space will not be elaborated upon here.

3. Hysteretic behaviour of ductile materials described by the Preisach model

This section is devoted to one-dimensional hysteresis behaviour of ductile (elasto-plastic) materials. Material response is modeled by various series or parallel connections of elastic (spring) and plastic (slip) elements. The accent is placed on the Preisach based analysis, which in comparison with traditional mechanics analysis ([Iwan, 1967]; [Asaro, 1975]) has advantage of simplicity and rigorous mathematical structure.

3.1. Parallel connection of elastic and slip element

A rigid-linearly hardening material behaviour (*Fig. 6a*) can be modeled by a parallel connection of slip (Saint-Venant) and elastic (spring-Hookean) element [Reiner, 1958].

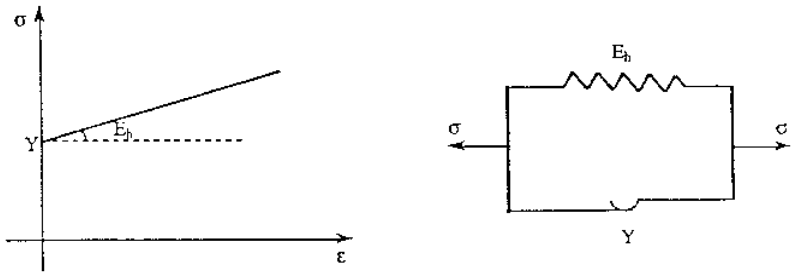

Fig. 6. — (*a*) Rigid-linearly hardening behaviour with initial yield stress Y and hardening modulus E_h; (*b*) Parallel connection of elastic and slip elements replicating the stress-strain behaviour in (*a*).

The yield (slip) strength of the slip element is $\pm Y$ (in tension and compression). The elastic modulus of the elastic element is E_h (*Fig. 6b*). The major hysteresis loop and several typical transition curves (straight lines) defining the strain output $\varepsilon(t)$, for the stress variation input $\sigma(t)$ between some extreme values σ_0 and $-\sigma_0$, are as shown in Figure 7. An appropriate Preisach function $P(\alpha, \beta)$ must be constructed to represent this hysteresis nonlinearity by the Preisach model. This can be accomplished using formula (4). Indeed, if the stress input is α, the strain output along the ascending branch of the major loop is $f_\alpha = (\alpha - Y)/E_h$. When the input is decreased along the transition curve shown in Figure 7 to some value β, the corresponding output is

$$f_{\alpha,\beta} = \frac{1}{2}(\beta + Y), \qquad -\sigma_0 \leqq \beta \leqq \sigma_0 - 2Y, \quad \beta + 2Y \leqq \alpha \tag{5}$$

and $f_{\alpha,\beta} = f_\alpha$, otherwise. Hence

$$\frac{\partial f_{\alpha,\beta}}{\partial \beta} = -\frac{1}{E_h} H(\alpha - \beta - 2Y), \tag{6}$$

where H denotes the Heaviside function. Consequently, the Preisach function is from (4)

$$P(\alpha, \beta) = \frac{1}{2E_h}\,\delta(\alpha - \beta - 2Y), \tag{7}$$

with δ being the Dirac delta function. Therefore, the Preisach function has support only along the line $\alpha - \beta = 2Y$ and is zero in the rest of the limiting triangle (*Fig. 8*). (In general, it can be shown that every hysteresis nonlinearity with a local memory, which can be represented by the Preisach model, has a Preisach function with support along a

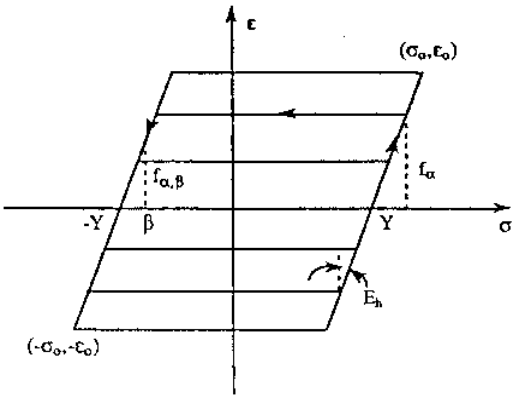

Fig. 7. — Major hysteresis loop and several transition lines, corresponding to the material model sketched in Figure 6. $\varepsilon - f_\alpha$ is the output value at the input $\sigma = \alpha$ along the ascending branch of the major loop, from which reversal has occured along transition line to input $\sigma = \beta$ and corresponding output $\varepsilon = f_{\alpha,\beta}$.

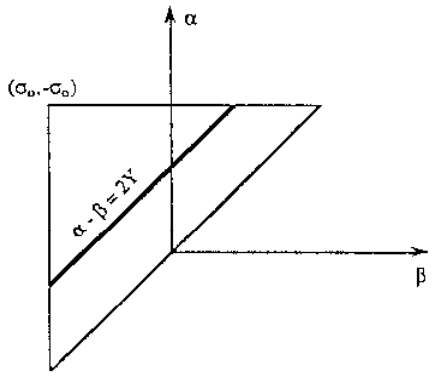

Fig. 8. — The Preisach function $P(\alpha, \beta)$ of the hysteresis nonlinearity in Figure 7 has support only along the line $\alpha - \beta = 2Y$, and is zero in every other point of the limiting triangle.

particular curve). Substitution of (7) into (1), leads to the strain output

$$\varepsilon(t) = \frac{1}{2E_h} \int_{2Y-\sigma_0}^{\sigma_0} G_{\alpha,\alpha-2Y}\, \sigma(t)\, d\alpha, \tag{8}$$

corresponding to an arbitrary but prescribed variation of stress input $\sigma(t)$.

Total strain for a system of infinitely many elements (units) of unequal yield strength, connected in a series (*Fig.* 9) is

$$\varepsilon(t) = \int_{Y_{min}}^{Y_{max}} p(Y)\, \varepsilon(Y, t)\, dY. \tag{9}$$

In (9) $\varepsilon(Y, t)$ is the strain corresponding to an individual unit with yield strength $Y_{min} \leqq Y \leqq Y_{max}$, given by the right-hand side of Eq. (8), and $p(Y)$ is the yield strength

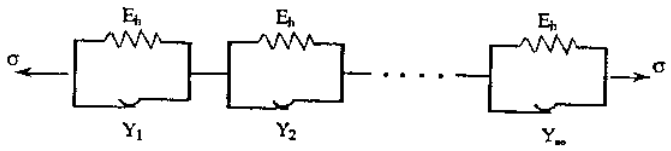

Fig. 9. – Series connection of infinitely many elementary units shown in Figure 6*b*. Each unit has identical hardening modulus, but different yield strength.

probability density function. Assume uniform distribution of yield strength

$$p(Y)=\frac{1}{Y_{max}-Y_{min}}=\text{Const.} \tag{10}$$

Substitution of (10) into (9), in conjunction with (8), leads to

$$\varepsilon(t)=\frac{1}{2E_h}\frac{1}{Y_{max}-Y_{min}}\int_{Y_{min}}^{Y_{max}}\int_{2Y-\sigma_0}^{\sigma_0} G_{\alpha,\alpha-2Y}\,\sigma(t)\,d\alpha\,dY. \tag{11}$$

Expression (11) can be more conveniently rewritten as

$$\varepsilon(t)=\frac{1}{4E_h}\frac{1}{Y_{max}-Y_{min}}\iint_A G_{\alpha,\beta}\,\sigma(t)\,d\alpha\,d\beta, \tag{12}$$

where the integration domain A is the area of the shaded band of the limiting triangle, shown in Figure 10. All $G_{\alpha,\beta}$ operators outside this band are inactive, and the Preisach

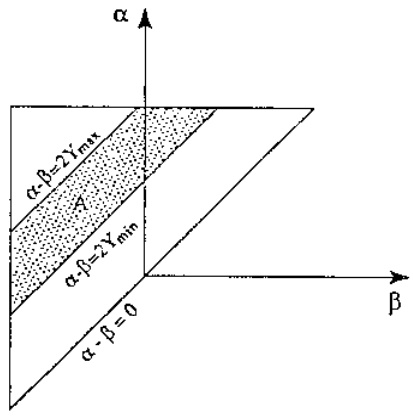

Fig. 10. – The Preisach function corresponding to material model of Figure 9 is supported only within the band area A, and is zero in the rest of the limiting triangle. Y_{min} and Y_{max} are the minimum and maximum yield strengths of elementary units shown in Figure 9.

function can be written as

$$P(\alpha, \beta) = \frac{1}{4E_h} \frac{1}{Y_{max} - Y_{min}} [H(\alpha + \beta - 2Y_{min}) - H(\alpha - \beta - 2Y_{max})], \tag{13}$$

where, as before, H denotes the Heaviside function.

3.2. Series connection of elastic and slip element

Elastic-ideally plastic material behaviour, sketched in the stress-strain curve plotted in Figure 11 *a*, can be modeled by a slip element (of yield strength Y) in a series connection

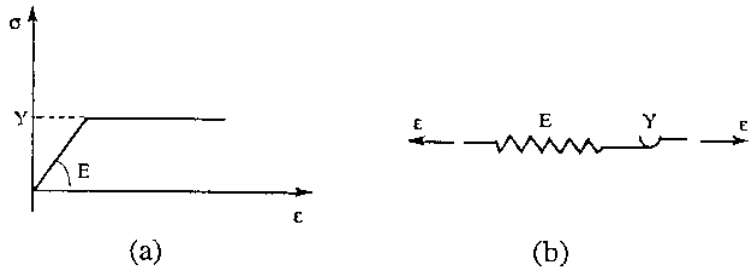

Fig. 11. – (*a*) Elastic-ideally plastic stress-strain behaviour with elastic modulus E and yield stress Y; (*b*) Series connection of elastic and slip elements reproducing the stress-strain behaviour in (*a*).

with an elastic element (of modulus E), Figure 11 *b*. To formulate the Preisach representation for the hysteresis behaviour of this material, consider the strain input variation $\varepsilon(t)$ ranging between extreme values ε_0 and $-\varepsilon_0$. From the major hysteresis loop and transition curves (straight lines), shown in Figure 12, it then follows that $f_\alpha = Y$,

$$f_{\alpha,\beta} = Y - E(\alpha - \beta), \qquad \alpha - 2\frac{Y}{E} \leqq \beta \leq \alpha \tag{14}$$

and $f_{\alpha,\beta} = -Y$, if $\beta \leq \alpha - 2Y/E$. Also, if $\beta \geqq \alpha$, $f_{\alpha,\beta} = Y$. To derive the Preisach function, differentiate (14) with respect to β

$$\frac{\partial f_{\alpha,\beta}}{\partial \beta} = E\left[H(\alpha - \beta) - H\left(\alpha - \beta - 2\frac{Y}{E}\right)\right], \tag{15}$$

and substitute (15) into (4)

$$P(\alpha, \beta) = \frac{E}{2}\left[\delta(\alpha - \beta) - \delta\left(\alpha - \beta - 2\frac{Y}{E}\right)\right]. \tag{16}$$

In this case the Preisach function has support along two parallel lines: $\alpha - \beta = 0$ and $\alpha - \beta = 2Y/E$ (*Fig.* 13), and is zero in the rest of the limiting triangle. The line $\alpha - \beta = 0$ is associated with the elastic, and line $\alpha - \beta = 2Y/E$ with the slip part of the connection.

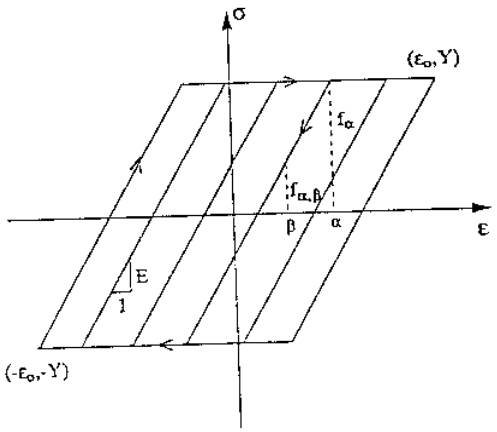

Fig. 12. – Major hysteresis loop and several transition lines, corresponding to the material model in Figure 11. $\sigma = f_\alpha$ is the output value at input $\varepsilon = \alpha$ along the major loop, from which reversal has occured along transition line to input $\varepsilon - \beta$ and corresponding output $\sigma = f_{\alpha,\beta}$.

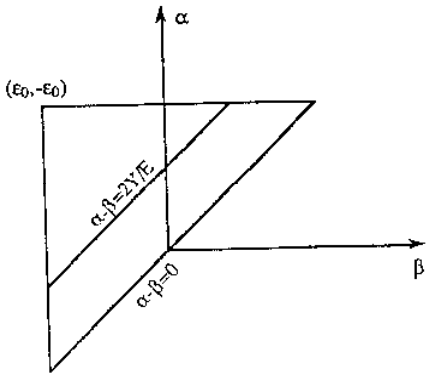

Fig. 13

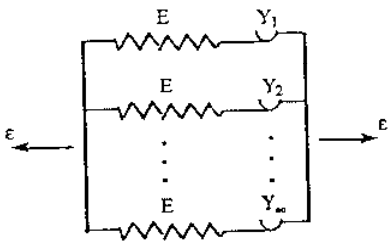

Fig. 14

Fig. 13. – The Preisach function $P(\alpha, \beta)$ of the hysteresis nonlinearity in Figure 12 is supported only along two parallel lines: $\alpha - \beta = 0$ and $\alpha - \beta = 2Y/E$, and is zero in every other point of the limiting triangle.

Fig. 14. Parallel connection of infinitely many elementary units shown in Figure 11 *b*. Each unit has identical elastic modulus, but different yield strength.

Substitution of (16) into (1), provides the expression for stress

$$\sigma(t) = \frac{E}{2}\left[\int_{-\varepsilon_0}^{\varepsilon_0} G_{\alpha,\alpha}\,\varepsilon(t)\,d\alpha - \int_{2(Y/E)-\varepsilon_0}^{\varepsilon_0} G_{\alpha,\alpha-2(Y/E)}\,\varepsilon(t)\,d\alpha\right], \tag{17}$$

corresponding to an arbitrary, prescribed variation of the strain input $\varepsilon(t)$.

For a system consisting of infinitely many of these elements (with unequal yield strength) connected in parallel (*Fig.* 14), the overall stress is

$$\sigma(t) = \int_{Y_{min}}^{Y_{max}} p(Y)\,\sigma(Y, t)\,dY. \tag{18}$$

Here, $\sigma(Y, t)$ is the stress in an individual element (unit) having yield strength within the range $Y_{min} \leqq Y \leqq Y_{max}$, as defined by the right-hand side of eq. (17). As before, $p(Y)$ is the yield strength probability density function. Assuming $p(Y)$ to be constant (10), from (18) it follows

$$(19)\quad \sigma(t) = \frac{E}{2}\left[\int_{-\varepsilon_0}^{\varepsilon_0} G_{\alpha,\alpha}\,\varepsilon(t)\,d\alpha - \frac{1}{Y_{max}}\,Y_{min}\int_{Y_{min}}^{Y_{max}}\int_{2(Y/E)-\varepsilon_0}^{\varepsilon_0} G_{\alpha,\alpha\ 2(Y/E)}\,\varepsilon(t)\,d\alpha\,dY\right].$$

Thus

$$(20)\qquad \sigma(t) = \frac{E}{2}\left[\int_{-\varepsilon_0}^{\varepsilon_0} G_{\alpha,\alpha}\,\varepsilon(t)\,d\alpha \quad \frac{E}{2}\,\frac{1}{Y_{max}-Y_{min}}\iint_A G_{\alpha,\beta}\,\varepsilon(t)\,d\alpha\,d\beta\right],$$

where the integration domain A is the area of the shaded band of the limiting triangle (*Fig.* 15). The associated Preisach function for the entire system is clearly

$$(21)\quad P(\alpha,\beta) = \frac{E}{2}\left\{\delta(\alpha-\beta) - \frac{E}{2}\,\frac{1}{Y_{max}-Y_{min}} \times\left[H\left(\alpha-\beta-2\frac{Y_{min}}{E}\right)\quad H\left(\alpha-\beta-2\frac{Y_{max}}{E}\right)\right]\right\}.$$

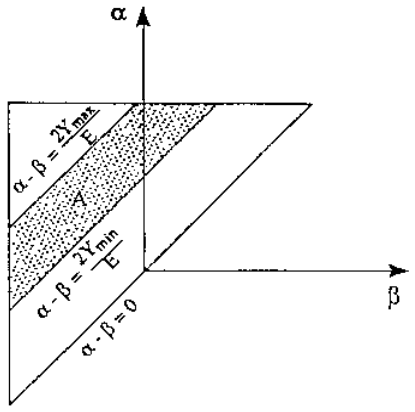

Fig. 15. The Preisach function corresponding to material model of Figure 14 has support along the line $\alpha-\beta=0$ and within the band area A, and is zero in the rest of the limiting triangle. Y_{min} and Y_{max} are the minimum and maximum yield strengths of elementary units shown in Figure 14.

The model of material behaviour represented by parallel connection of elastic-ideally plastic elements has been often studied in the wake of the early work by [M, 1926]. Individual elements can be taught to represent the individual grains in a random polycrystalline agregate. Grains most favorably oriented for slip correspond to the weakest element, *i.e.* the element with the lowest value of the yield strength Y. Since each grain is subjected to identical average stress, and since the exact position of grains (elements) within the system is irrelevant, the parallel bar model is a discrete version of the self-consistent model [Hill, 1965]. In order words, the response of each bar depends

on the state of the other bars only through their contribution to the effective (overall) system moduli.

3.3. A THREE-ELEMENT UNIT

Elastic-linearly hardening material behaviour, characterized by the stress-strain curve shown in Figure 16*a* (E and E_h are elastic and hardening moduli), can be replicated by

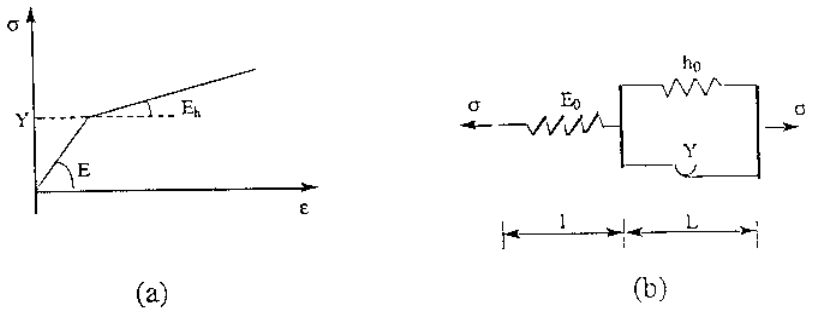

Fig. 16. (*a*) Elastic-linearly hardening stress-strain behaviour with elastic modulus E, initial yield stress Y and hardening modulus E_h; (*b*) Three-element unit reproducing the stress-strain behaviour in (*a*). $E=E_0(l+L)/l$, $E_h=Eh/(E+h)$ and $h=h_0(l+L)/L$.

a three-element unit shown in Figure 16*b*. Elastic element of length l and modulus E_0 is connected in a series with a parallel connection of elastic and slip element, of length L, modulus h_0 and yield strength Y. It then follows that $E=E_0(l+L)/l$ and $E_h=Eh/(E+h)$, where $h=h_0(l+L)/L$. The Preisach function can be determined from the hysteresis nonlinearity shown in Figure 17, which relates the stress input to strain output. The

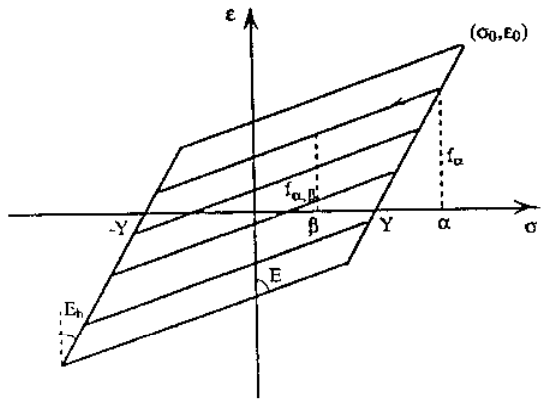

Fig. 17. - Major hysteresis loop and several transition lines, corresponding to the material model in Figure 16. $\varepsilon=f_\alpha$ is the output value at input $\sigma=\alpha$ along the major loop, from which reversal has occured along transition line to the input $\sigma=\beta$ and corresponding output $\varepsilon=f_{\alpha,\beta}$.

Preisach function in this case has support along the lines $\alpha-\beta=0$ and $\alpha-\beta=2Y$, *i.e.* it

is given by

$$P(\alpha, \beta) = \frac{1}{2E}\left[\delta(\alpha-\beta) + \frac{E-E_h}{E_h}\delta(\alpha-\beta-2Y)\right]. \tag{22}$$

The expression for strain as a function of applied stress is, consequently,

$$\varepsilon(t) = \frac{1}{2E}\left[\int_{-\sigma_0}^{\sigma_0} G_{\alpha,\alpha}\,\sigma(t)\,d\alpha + \frac{E-E_h}{E_h}\int_{2Y-\sigma_0}^{\sigma_0} G_{\alpha,\alpha-2Y}\,\sigma(t)\,d\alpha\right]. \tag{23}$$

The first and second term on the right-hand side of (23) are elastic and plastic strain, respectively. For a system consisting of infinitey many of three-element units, connected in a series and with uniform yield strength distribution within the range $Y_{min} \leqq Y \leqq Y_{max}$, the total strain is

$$\varepsilon(t) = \frac{1}{2E}\left[\int_{\sigma_0}^{\sigma_0} G_{\alpha,\alpha}\,\sigma(t)\,d\alpha + \frac{E-E_h}{2E_h}\frac{1}{Y_{max}-Y_{min}}\iint_A G_{\alpha,\beta}\,\sigma(t)\,d\alpha\,d\beta\right]. \tag{24}$$

In (24) the integration domain A is the area of the band contained between the lines $\alpha-\beta=2Y_{min}$ and $\alpha-\beta=2Y_{max}$ in the limiting triangle. The first term on the right-hand side of (24) is the elastic strain, which can be written as $\sigma(t)/E$.

In the case when the strain is the input and stress output, the Preisach function becomes

$$P(\alpha, \beta) = \frac{E}{2}\delta(\alpha-\beta) - \frac{1}{2}(E-E_h)\,\delta\left(\alpha-\beta-2\frac{Y}{E}\right). \tag{25}$$

The stress expression is from (1)

$$\sigma(t) = \frac{E}{2}\int_{-\varepsilon_0}^{\varepsilon_0} G_{\alpha,\alpha}\,\varepsilon(t)\,d\alpha - \frac{1}{2}(E-E_h)\int_{2(Y/E)-\varepsilon_0}^{\varepsilon_0} G_{\alpha,\alpha-2(Y/E)}\,\varepsilon(t)\,d\alpha. \tag{26}$$

If infinitely many three-element units, with a uniform distribution of yield strength (10), are connected in parallel (*Fig.* 18), the overall stress is from (26)

$$\sigma(t) = \frac{E}{2}\left[\int_{-\varepsilon_0}^{\varepsilon_0} G_{\alpha,\alpha}\,\varepsilon(t)\,d\alpha - \frac{1}{2}(E-E_h)\frac{1}{Y_{max}-Y_{min}}\iint_A G_{\alpha,\beta}\,\varepsilon(t)\,d\alpha\,d\beta\right]. \tag{27}$$

The integration domain A in (27) is the area of the band contained between the lines $\alpha-\beta=2Y_{min}/E$ and $\alpha-\beta=2Y_{max}/E$ in the limiting triangle.

3.4. Some examples

To illustrate the application of the Preisach model the stress-strain hysteresis curves are here determined for material models introduced in the previous subsections. Various cyclic stress and strain input hystories are considered. In each case the loading or straining starts from zero stress and strain state. The limiting triangle is then initially

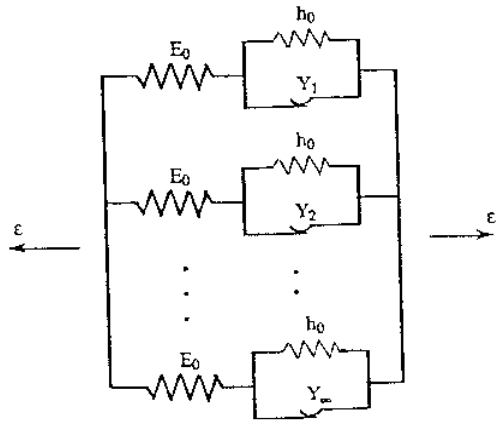

Fig. 18. - Parallel connection of infinitely many three-element units.
Each unit has identical elastic and hardening moduli, but different yield strength.

divided into two equal parts, as in Figure 19*b*. The interface line between these parts is the line $\alpha+\beta=0$. Bellow this line all $G_{\alpha,\beta}$ operators have positive, and those above negative outputs.

Figure 19*a* shows hysteretic behaviour of the parallel-bar model from Figure 14, corresponding to the cyclic strain variation input as in Figure 19*b*. Computation is performed for the case $Y_{max}=4\,Y_{min}$, rendering the ultimate stress that this material can sustain $(Y_{min}+Y_{max})/2=2.5\,Y_{min}$. The corresponding strain is $\varepsilon_0=Y_{max}/E=4\,\varepsilon_e$, where $\varepsilon_e=Y_{min}/E$ is the elastic limit strain. Initial configuration of the limiting triangle is shown in Figure 19*c*. The band area A from Figure 15 in this case is, therefore, just the area of the shaded triangle. Clearly, for $\varepsilon=0$, Eq. (20) requires that $\sigma=0$. When the strain is

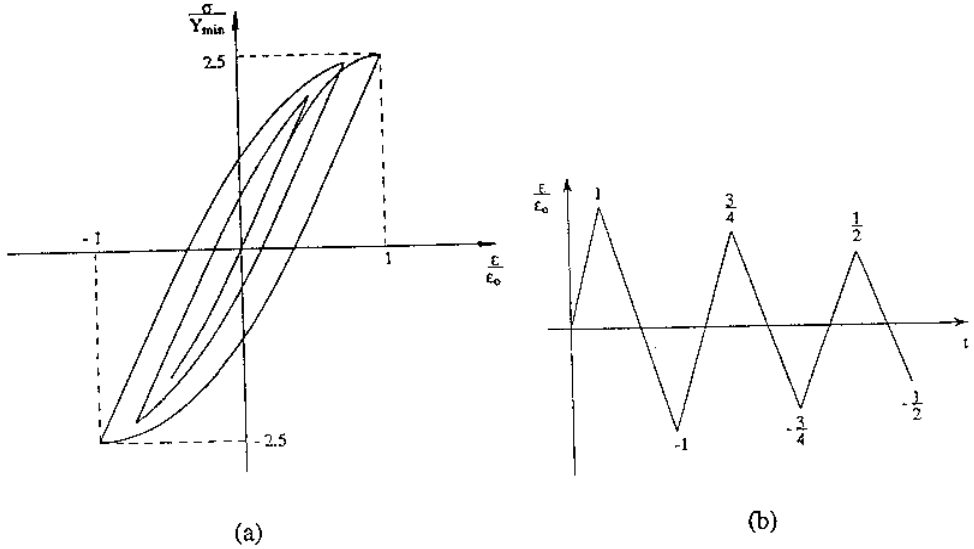

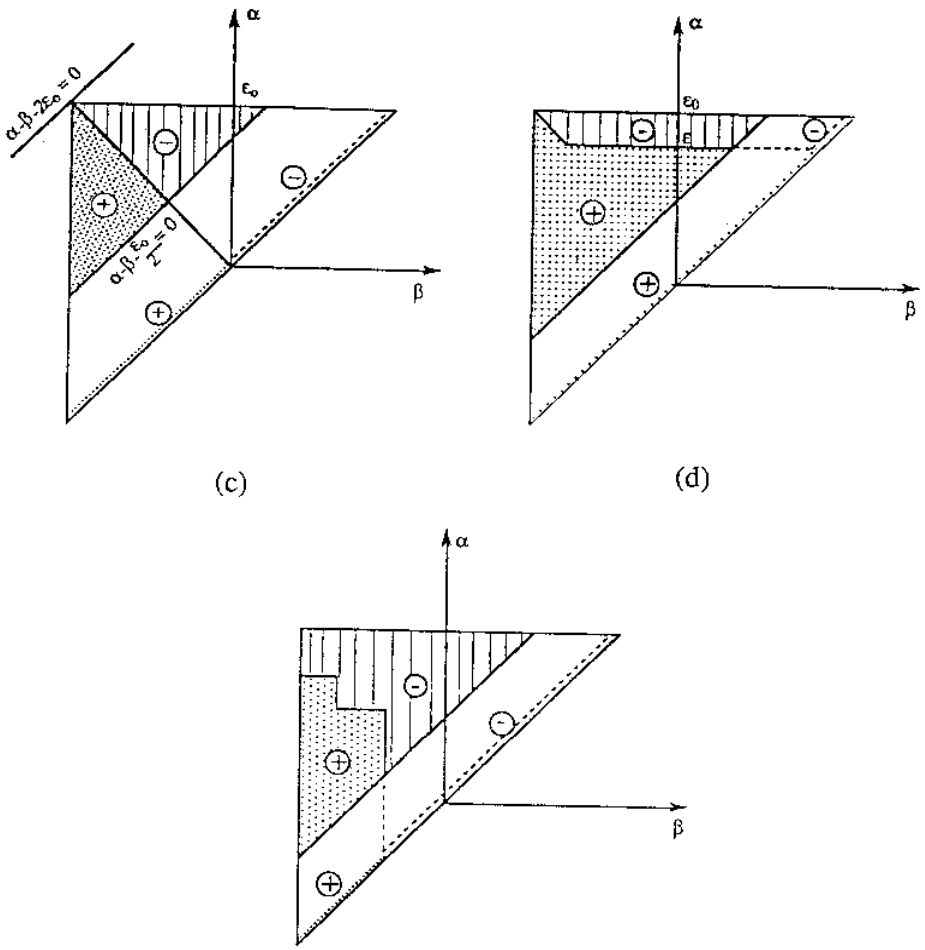

Fig. 19. – (*a*) Hysteretic behaviour of the parallel-bar model shown in Figure 14; (*b*) Corresponding strain input variation; (*c*) Initial configuration of the limiting triangle; (*d*) Configuration of the limiting triangle corresponding to the strain increase to value $\varepsilon<\varepsilon_0$; (*e*) Final configuration of the limiting triangle, at the instant when the strain is cycled down to the value $-\varepsilon_0/2$.

increased to some value $\varepsilon\leqq\varepsilon_0$, the configuration of the limiting triangle is as shown in Figure 19*d*. By simple geometric considerations, from Eq. (20) it follows that the stress output is

$$\sigma = E\varepsilon - \frac{E^2}{2}\cdot\frac{1}{Y_{max}-Y_{min}}\cdot\left(\varepsilon-\frac{Y_{min}}{E}\right)^2 = E\varepsilon-\frac{2}{3}\frac{E}{\varepsilon_0}(\varepsilon-\varepsilon_e)^2. \tag{28}$$

Analysis proceeds in a straightforward manner for any strain variation input, such as one in Figure 19*b*. The configuration of the limiting triangle at the instant when the strain is cycled down to the value $-\varepsilon_0/2$ is shown in Figure 19*e*.

The obtained hysteretic behaviour (*Fig.* 19*a*) is same as that of the well-known Masing sub-element model. In particular, if the stress-strain curve on primary loading has an equation $\sigma = g(\varepsilon)$, on unloading the corresponding portion of the stress-strain curve has the equation $\sigma' = g((1/2)\varepsilon')$, where (σ', ε') are the new coordinates eminating from the point of unloading.

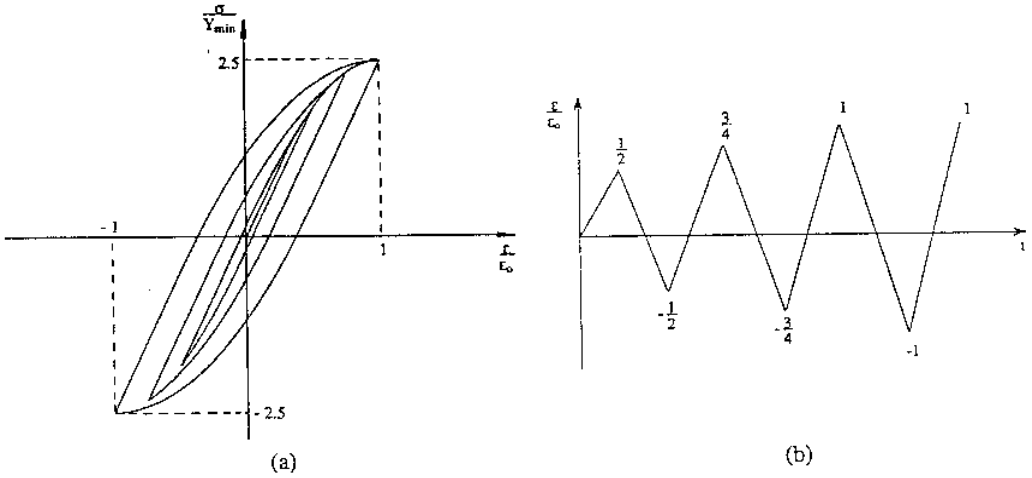

Fig. 20. – Hysteretic behaviour of the same material mode as for Figure 19, but for the strain input shown in Figure 20*b*.

Figure 20*a* shows the hysteretic behaviour of the same material model, but for the strain variation input shown in Figure 20*b*. This example is selected to illustrate the previously discussed wiping-out property of the Preisach model. Namely, the final-major hysteresis loop (corresponding to the extreme strain input variation between ε_0 and $-\varepsilon_0$, and back) is not influenced by previous cycles of lower strain variation, *i.e.* the inner (minor) hysteretic loops.

Solid line curves in Figure 21*a* represent hysteretic behaviour of the material model consisting of a series connection of an infinite number of tree-element units shown in Figure 16*b*. The cyclic input stress variation is shown in Figure 21*b*. During primary loading, elastic behavior ceases at the stress level Y_{min}, at which the yield strength of the weakest slip element is exceeded. The nonlinear behavior becomes more apparent as more slip elements are activated. From Eq. (24) it follows

$$\varepsilon = \frac{\sigma}{E} + \frac{E - E_h}{2EE_h} \frac{1}{Y_{max} - Y_{min}} (\sigma - Y_{min})^2. \tag{29}$$

The nonlinear behavior persists until the strongest slip element is activated, which occurs at the stress level Y_{max}. The stress-strain curve associated with further loading is linear,

with a constant (saturation) hardening rate E_h. The strain level at the begining of the saturated state is clearly

$$\varepsilon_0 = \frac{1}{E}\,\frac{Y_{max}+Y_{min}}{2} + \frac{1}{E_h}\,\frac{Y_{max}-Y_{min}}{2}. \tag{30}$$

The nonlinear range is confined within the strain interval

$$\varepsilon_0 - \varepsilon_e = (Y_{max}-Y_{min})(E+E_h)/2EE_h.$$

The dashed lines in Figure 21 *c* correspond to the loading response of a single three-element unit, with the (average) yield strength $(Y_{max}+Y_{min})/2$.

Figure 21 *d* shows the initial configuration of the limiting triangle used in calculation of the hysteretic behaviour presented in Figure 21 *a*. It was assumed that $Y_{max}=2\,Y_{min}$ and $E_h=E/9$, while the maximum stress input was taken to be $\sigma_0=2.5\,Y_{min}$. The range of the nonlinear hardening during the primary loading is $\varepsilon_0 - \varepsilon_e=5\varepsilon_e$ in strain, and $Y_{max}-Y_{min}$ in stress. During unloading the nonlinear range is twice as big, in both stress and strain. This is an obvious consequence of the nature of the slip elements, having elastic range between tension and compression 2Y. Geometrically, this is also clear from the limiting triangle of the Preisach model. During unloading the triangular part of the band area, which gives the nonlinear input-output behaviour, is twice as big as the corresponding triangular part during the primary loading (T and 2T in *Fig.* 21 *e* and *f*). From the limiting triangle it also follows that the elastic range during unloading ($2\,Y_{min}$) is twice as big as during the primary loading from zero stress (Y_{min}). Finally, observe

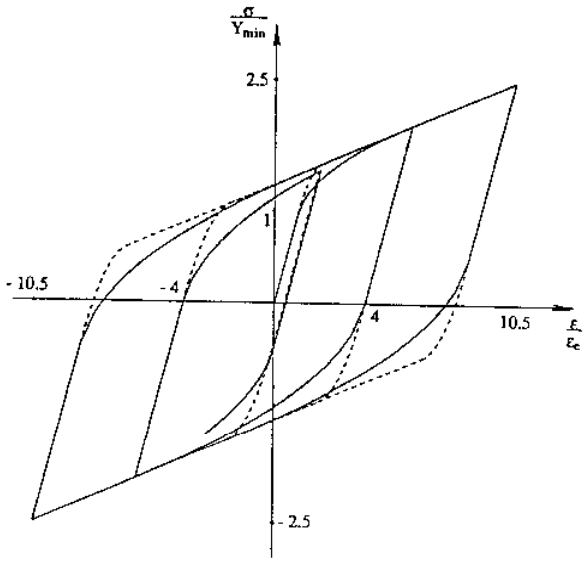

(a)

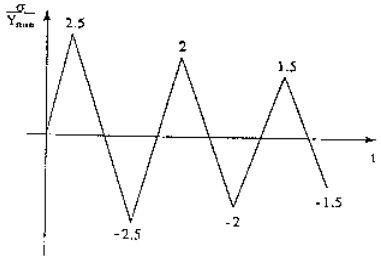

(b)

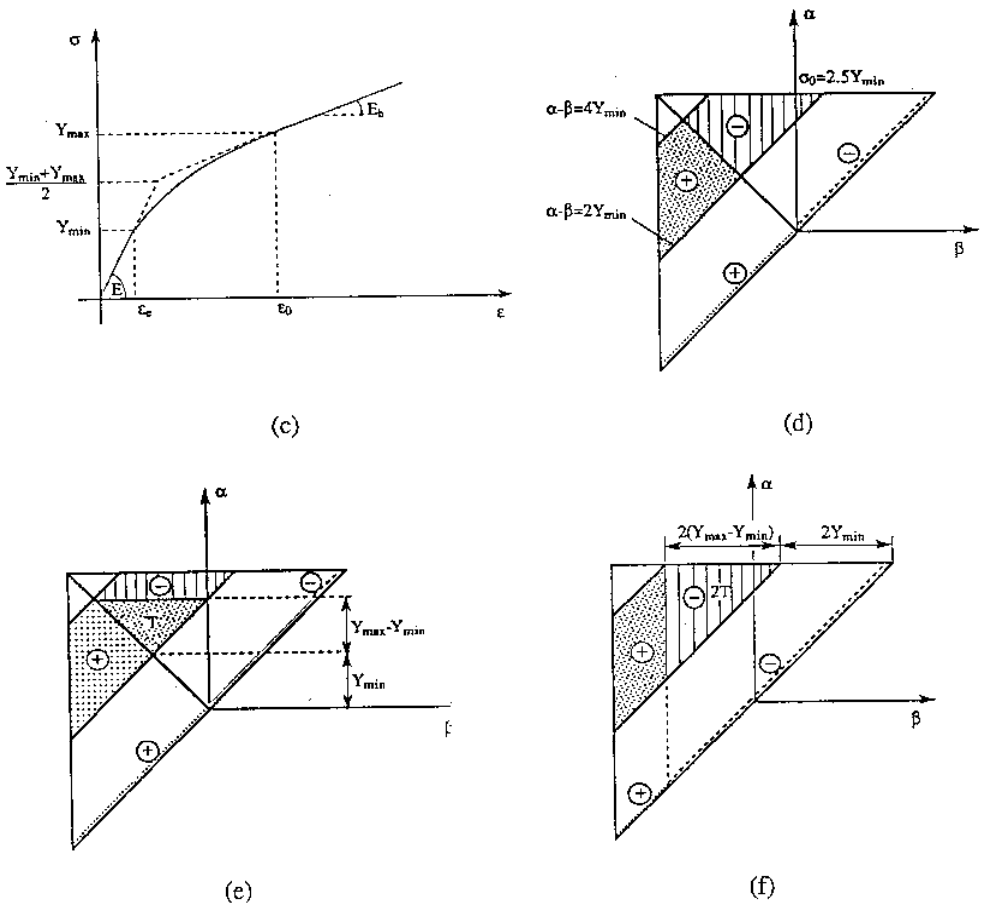

Fig. 21. (*a*) Hysteretic behaviour of series (solid line) and parallel (dashed line) connection of three-element units shown in Figure 16*b*; (*b*) Stress variation input for the series connection model; (*c*) Stress-strain behaviour during the primary loading (series connection); (*d*) Initial configuration of the limiting triangle; (*e*) Triangular part T giving rise to the nonlinear part of the stress-strain curve during primary loading; (*f*) Triangular part 2T giving rise to the nonlinear part of the stress-strain curve during unloading.

that after the stress level Y_{max} is reached in primary loading, further increments of stress $\Delta\sigma$ are accompanied with equal increments of the band area of the limiting triangle [parallelegrams of area $(2(Y_{max}-Y_{min})\Delta\sigma]$, hence the resulting linear behaviour and constant hardening rate. Similar observation applies to unloading or any subsequent reloading.

Dashed line curves in Figure 21 *a* represent hysteretic behaviour of the material model represented by an infinite number of three-element units connected in parallel, as shown in Figure 18. During the primary loading, nonlinear behaviour sets in at the stress level

Y_{min} and is governed by a quadratic stress-strain relationship

$$\sigma = E\varepsilon - \frac{E}{2}(E - E_h)\frac{1}{Y_{max} - Y_{min}}\left(\varepsilon - \frac{Y_{min}}{E}\right)^2. \tag{31}$$

This nonlinear range extends untill strain level $\varepsilon_0 = Y_{max}/E$, when the strongest slip element begins to yield. The corresponding overall stress is

$$\sigma_0 = \frac{Y_{max} + Y_{min}}{2} + \frac{E_h}{E}\frac{Y_{max} - Y_{min}}{2}. \tag{32}$$

Dashed lines in Figure 22 *a* correspond to the loading behaviour of a single three-element unit with the (average) yield strength $(Y_{min} + Y_{max})/2$.

Hysteretic behaviour shown by the dashed line curves in Figure 21 *a* is obtained using identical material parameters as for the series connection of three-element units, *i.e.* $E_h = E/9$ and $Y_{max} = 2\,Y_{min}$. For the sake of direct comparison of two material models, the strain output obtained in a series connection is taken as the strain input in parallel connection (*Fig.* 22 *c*). Initial configuration of the corresponding limiting triangle is shown in Figure 22 *b*. The nonlinear transition region, separating linear elastic (E) and constant hardening (E_h) regions, has a smaller range than for the parallel connection, since $E_h < E$. In fact, from (30) and (32), the nonlinear ranges for parallel and series connection are related via

$$(\varepsilon_0 - \varepsilon_e)_{par} = \frac{2E_h}{E + E_h}(\varepsilon_0 - \varepsilon_e)_{ser}, \tag{33}$$

and

$$(\sigma_0 - \sigma_e)_{par} = \frac{E + E_h}{2E}(\sigma_0 - \sigma_e)_{ser}. \tag{34}$$

For example, for the case of Figure 21 *a*, with $E_h = E/9$, the strain range during nonlinear transition region is 5 times larger in a series connection than in a parallel connection. The stress range is 1.8 times larger. Physically, this is clear since in the parallel connection of three-element units, the overall stress is only the average of stresses in the individual units. Hence, when the strongest slip element is activated, at its stress level Y_{max}, the overall stress σ is far bellow Y_{max} stress level. On the other hand, in a seires connection the overall stress is exactly equal to stress Y_{max}, required to activate the strongest slip element.

4. Hysteretic energy dissipation and locked-in energy

Consider a rectangular loop of the elementary hysteresis operator shown in Figure 1. For a cyclic input variation along all the loop, the energy dissipation is equal to the area enclosed by the loop, *i.e.* $2(\alpha - \beta)$. This energy dissipation is a consequence of the

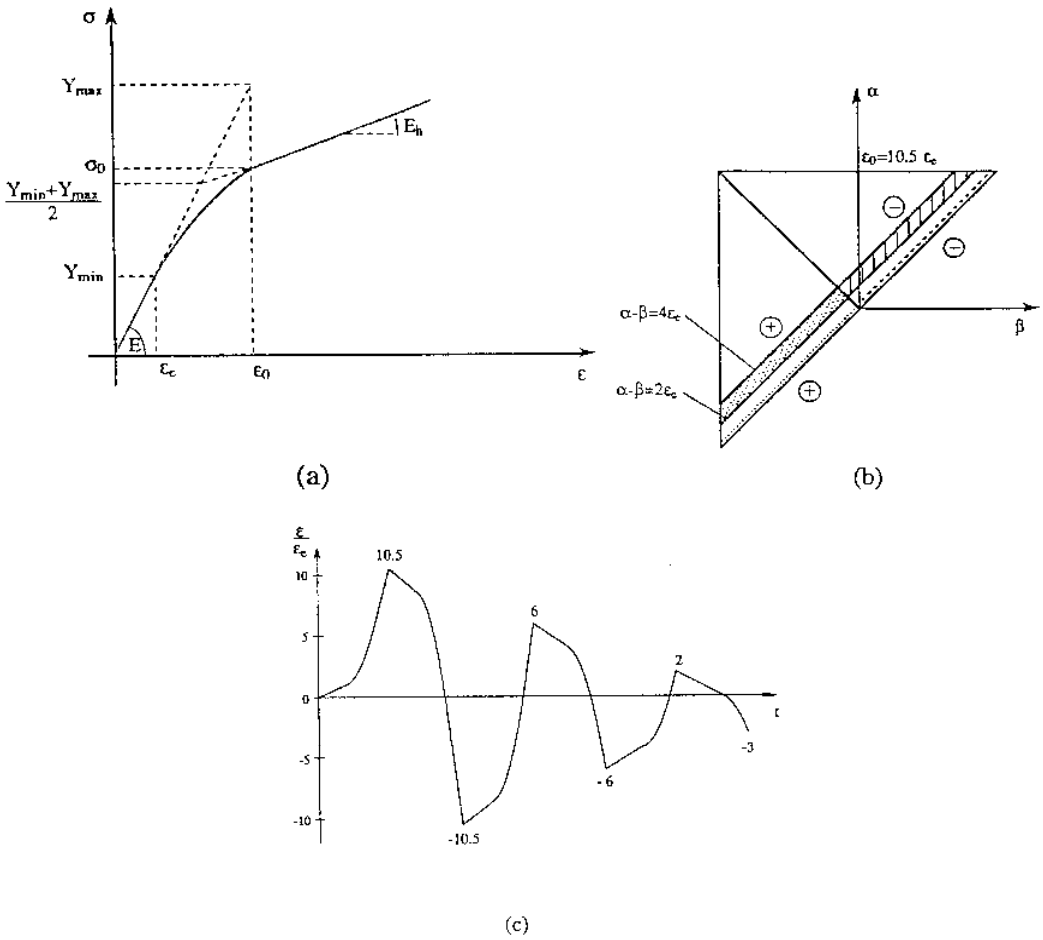

Fig. 22. — (*a*) Stress-strain behaviour during the primary loading of a parallel connection of three-element units, shown in Figure 16*b*; (*b*) Initial configuration of the limiting triangle for the parallel connection; (*c*) Strain input variation for the parallel connection, obtained as the strain output of previously considered series connection.

irreversible processes occuring during switching-up and -down portions of the rectangular loop. Assuming that these processes are of the same nature, energy dissipation during one switching is $(\alpha-\beta)$. Therefore, if Ω denotes the region of the limiting triangle for which the elementary operators represented by points (α, β) were switched during some input variation, the corresponding energy dissipation is

$$Q=\iint_{\Omega} |\mathbf{P}(\alpha, \beta)|(\alpha-\beta)\,d\alpha\,d\beta. \tag{35}$$

Consider, for example, the material model represented by a series connection of an infinite number of three-element units. The stress-strain expression during the primary

loading from initial (intact) state is given by Eq. (29) and is ploted in Figure 21 *c*. Substructing from (29) the elastic component of strain gives

$$\varepsilon_p = \frac{1}{2h}\frac{(\sigma - Y_{min})^2}{Y_{max} - Y_{min}}, \qquad h = \frac{EE_h}{E - E_h} \tag{36}$$

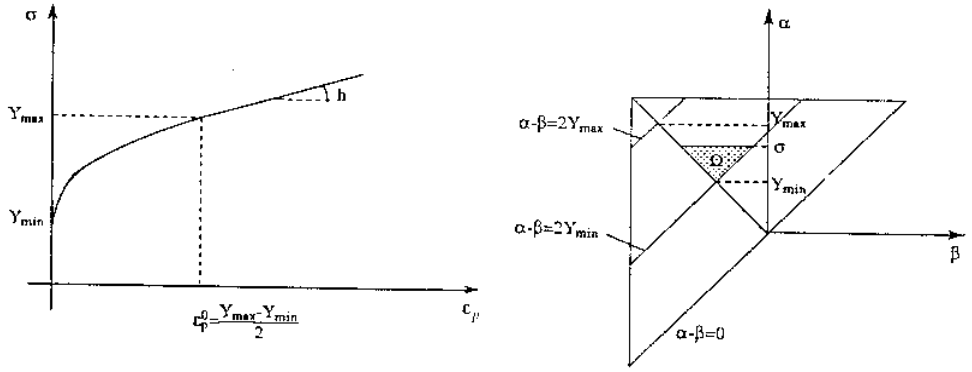

(a) (b)

Fig. 23 – (*a*) Stress-plastic strain curve of the material modeled by a series connection of three-element units. ε_p^0 is the plastic strain at the begining of linear hardening, with plastic modulus h; (*b*) Integration domain Ω of the limiting triangle used in the evaluation of energy dissipation corresponding to loading from zero to σ stress state.

plotted in Figure 23 *a*. The plastic work done, corresponding to stress level

$$Y_{min} \leq \sigma \leq Y_{max},$$

is

$$W_P = \sigma\varepsilon_p - \int_{Y_{min}}^{\sigma} \varepsilon_p \, d\sigma = \frac{1}{6h}\frac{(\sigma - Y_{min})^3}{Y_{max} - Y_{min}}\left(2 + \frac{3Y_{min}}{\sigma - Y_{min}}\right). \tag{37}$$

To determine the part of W_P dissipated into heat, use (35) in conjunction with the Preisach function

$$P(\alpha, \beta) = \frac{1}{2E}\delta(\alpha - \beta) + \frac{1}{4h}\left(\frac{1}{Y_{max}} - \frac{1}{Y_{min}}\right)[H(\alpha - \beta - 2Y_{min}) - H(\alpha - \beta - 2Y_{max})], \tag{38}$$

as required by (24). The integration domain Ω is shown in Figure 23 *b*. Substituting (38) into (35) therefore gives

$$Q = \frac{1}{4h}\left(\frac{1}{Y_{max}} - \frac{1}{Y_{min}}\right)\int_{Y_{min}}^{\sigma}\left[\int_{-\alpha}^{\alpha}{}^{2Y_{min}} (\alpha - \beta)\, d\beta\right] d\alpha, \tag{39}$$

i.e.

$$Q=\frac{1}{6h}\frac{(\sigma-Y_{min})^3}{Y_{max}-Y_{min}}\left(1+\frac{3Y_{min}}{\sigma-Y_{min}}\right). \tag{40}$$

The difference

$$W_L=W_P-Q=\frac{1}{6h}\frac{(\sigma-Y_{min})^3}{Y_{max}-Y_{min}} \tag{41}$$

is the locked-in energy stored within the system during the primary loading from initial, zero stress state to the state of stress $Y_{min}<\sigma\leq Y_{max}$.

If the loading reaches the stress level $\sigma>Y_{max}$:

$$W_P=W_P^0+\frac{1}{2h}(\sigma-Y_{max})(\sigma+Y_{max}) \tag{42}$$

$$Q=Q^0+\frac{1}{2h}(\sigma-Y_{max})(Y_{min}+Y_{max}) \tag{43}$$

$$W_L=W_L^0+\frac{1}{2h}(\sigma-Y_{max})(\sigma-Y_{min}), \tag{44}$$

where $(\ )^0$ are the values obtained from expressions (39), (40) and (41) corresponding to the stress level $\sigma=Y_{max}$. For example, since

$$\frac{Q^0}{W_P^0}=\frac{Y_{max}+2Y_{min}}{Y_{min}+2Y_{max}}, \tag{45}$$

it follows that for $Y_{max}=1.5\,Y_{min}$, the dissipated energy at the stress state $\sigma=Y_{max}$ is $Q^0=87.5\%\ W_P^0$, while the locked-in energy is $W_L^0=12.5\%\ W_P^0$.

The locked-in energy stored in a material is of direct significance in explaining the unloading and subsequent reloading behaviour. To illustrate this, consider unloading from the state $A(\varepsilon_0, Y_{max})$ to the state $B(-\varepsilon_*, -\sigma_*)$, such that the state $O(0, 0)$ is passed during subsequent reloading to state A, (*Fig. 24a*). In this case

$$\sigma_*=Y_{min}+(\sqrt{2}-1)(Y_{max}-Y_{min}),$$

provided that $Y_{max}\leqq(2+\sqrt{2})\,Y_{min}$ (so that $\sigma_*\leqq 2\,Y_{min}$). The question arises why the material behaves differently in loading from state O to state A, before and after the cycle

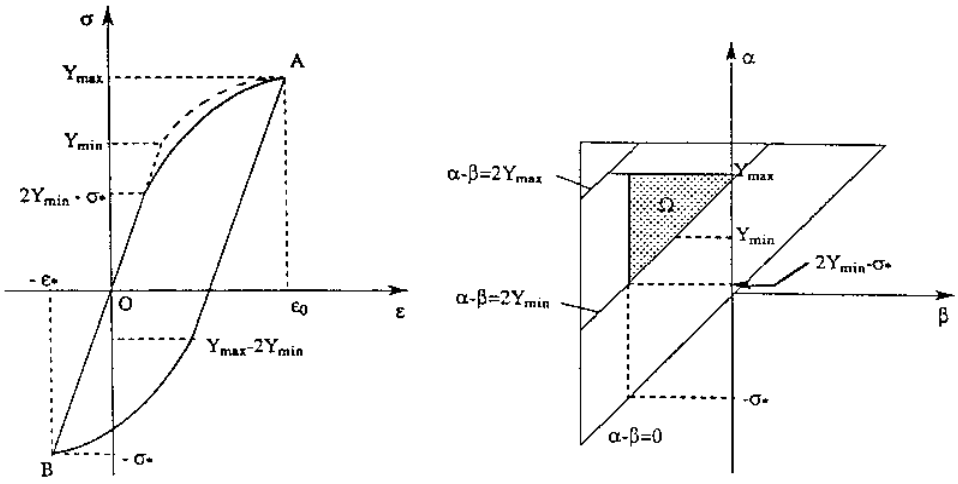

(a) (b)

Fig. 24. – (*a*) Dashed line part of the stress-strain curve corresponds to primary loading from O to A, while solid line between O and A corresponds to loading after the cycle OABO; (*b*) Integration domain Ω used in the evaluation of energy dissipation between A and B, or B and A.

OABO. The dashed curve in Figure 24*a* corresponds to primary loading and is described by Eq. 29), while the solid curve corresponds to loading after the cycle OABO and is described by equation

$$\varepsilon = \frac{\sigma}{E} + \frac{1}{4h}\frac{(\sigma - 2Y_{min} + \sigma_*)^2}{Y_{max} - Y_{min}}. \tag{46}$$

Plastic work expanded along this curve from O to A is

$$W_P^1 = \frac{1}{6h}(Y_{max} - Y_{min})^2\left(3\frac{Y_{max}}{Y_{max} - Y_{min}} - \sqrt{2}\right). \tag{47}$$

The part of this work dissipated into heat is equal to half the area of the solid line hysteresis loop in Figure 24*a*, since the nonlinear (dissipative) parts of the curve from A to B, and B to A are identical. Hence

$$Q^1 = \frac{1}{6h}(Y_{max} - Y_{min})^2\left(3\frac{Y_{min}}{Y_{max} - Y_{min}} + \frac{\sqrt{2}}{2}\right). \tag{48}$$

Expression (48) also follows from formula (35) applied to integration domain Ω shown in Figure 24*b*. Integrating

$$Q^1 = \frac{1}{4h}\frac{1}{Y_{max} - Y_{min}}\int_{2Y_{min} - \sigma_*}^{Y_{max}}\left[\int_{-\sigma_*}^{\alpha - 2Y_{min}}(\alpha - \beta)\,d\beta\right]d\alpha, \tag{49}$$

Eq. (48) is again arrived at.

The locked-in energy within the material during this second path OA is, therefore,

$$W_L^1 = W_P^1 - Q^1 = 3\left(1 - \frac{\sqrt{2}}{2}\right)\frac{1}{6h}(Y_{max} - Y_{min})^2. \tag{50}$$

The material in state A must have the same structure before and after the cycle ABA, since it responds to further loading or unloading and subsequent reloading in exactly the same way, before and after the cycle ABA. Consequently, the locked-in energy in state A, after the cycle ABA, has to be

$$W_L^0 = \frac{1}{6h}(Y_{max} - Y_{min})^2, \tag{51}$$

as before the cycle ABA (*Eq.* (41) with $\sigma = Y_{max}$). The difference

$$\Delta W_L = W_L^0 - W_L^1 = \left(3\frac{\sqrt{2}}{2} - 2\right)\frac{1}{6h}(Y_{max} - Y_{min})^2 \tag{52}$$

is, therefore, the locked-in energy in state O, after completing the cycle OABO. This locked-in energy, *i.e.* the locked-in microscopic stress field (having zero average), helps the macroscopic stress σ in reaching the state A, after the cycle OABO. This explains the departure from the original, dashed line curve of primary loading, and decrease in plastic work externaly required to deform material to state A. Note that ΔW_L is not merely $\Delta W_P = (W_P^0 - W_P^1)$, because the creation of the locked-in energy of amount ΔW_L during the primary loading is accompanied by the corresponding heat dissipation $\Delta Q = Q^0 - Q^1$. In fact:

$$\Delta W_P = (\sqrt{2} - 1)\frac{1}{6h}(Y_{max} - Y_{min})^2 \tag{53}$$

$$\Delta Q = \left(1 - \frac{\sqrt{2}}{2}\right)\frac{1}{6h}(Y_{max} - Y_{min})^2, \tag{54}$$

so that $\Delta W_L = \Delta W_P - \Delta Q$.

It is finally noted that considering the "symmetric" hysteresis loop, *i.e.* if the state B is obtained from state A by unloading to stress $-\sigma_* = -Y_{max}$ (*Fig.* 25), no net locked-in energy is accumulated during complete unloading from A to B, or reloading from B to A. In other words, the plastic work associated with unloading or reloading parts of the cycle ABA is all dissipated into heat

$$W_P^1 = Q^1. \tag{55}$$

This occurs since both the plastic work and the dissipated energy in the cycle ABA are equal to the area within the "symmetric" loop. Half of this area corresponds to unloading and half to reloading part. The locked-in energy in zero macroscopic stress state O_1 is

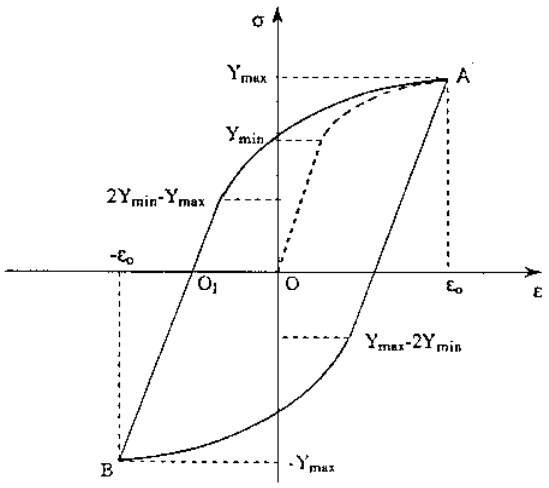

Fig. 25. If the hysteresis loop is "symmetric", no net locked-in energy is produced during complete unloading from A to B, or reloading from B to A. The locked-in energy in state O_1 is equal to the locked-in energy in state A, stored during the primary loading from O to A.

exactly equal to locked-in energy in state A, produced during the primary loading from O to A.

An analogous analysis of the dissipated and locked-in energy can be done for other material models, such as one of parallel connection shown in Figure 14 [Lubarda *et al.*, 1992].

5. Conclusion

The present paper focuses on the application of the Preisach model to the response of ductile solids subjected to cyclic stress or strain. Closed form analytical solutions for the hysteretic response were derived for several rheological models reminiscant to those commonly exploited in viscoelasticity. Main advantages of the proposed formulation are associated with its simple and rigorous mathematical structure allowing for analytical solutions, and precise evaluation of the energy dissipation including distinction between energy dissipated into heat and the locked-in energy. The method also leads to convenient identification of material parameters from experimental data and correlation to hardening characteristics and anisotropic response during unloading from the plastic state and reverse loading and reloading. Additional advantage of the model consists in its relationship to fatigue analysis, since the inherent features of the model, such as the wiping-out properties, can be related to corresponding cycle counting procedures, similar to the well known rainflow model.

Further extensions of the model are needed in order to address the three dimensional issues regarding the evolution of the yield surface and corresponding hardening rules (some of these are recently discussed in a paper by [White *et al.*, 1990]). Also, the modifications are needed for the analysis of brittle-ductile phenomena, by considering

the probability of brittle failure of individual elements leading eventually to a cascade mode of macro-failure.

Acknowledgments

This work was supported by the U.S.-Yugoslav Joint Fund for Scientific and Technological Coorporation, in cooperation with the NSF under Grant JF-991 (V.A.L.), and U.S. Department of Energy, Office of Basic Energy Sciences, Division of Engineering and Geosciences (D.S. and D.K.).

REFERENCES

ASARO R. J., 1975, Elastic-plastic memory and kinematic-type hardening, *Acta Met.*, **23**, 1255-1265.

BOWER A. F., 1989, Cyclic hardening properties of hard-drawn copper and rail steel, *J. Mech. Phys. Solids*, **37**, 455-470.

CONLE A., OXLAND T. R., TOPPER T. H., 1988, Computer-based prediction of cyclic deformation and fatigue behaviour, *Low Cycle Fatigue. ASTM STP* 942, 1218-1236.

DRUCKER D. C., PALGEN L., 1981, On stress-strain relations suitable for cyclic and other loading, *J. Appl. Mech.*, **48**, 479-485.

EVERETT D. H., WHITTON W. I., 1952, A general approach to hysteresis, *Trans. Faraday Soc.*, **48**, 749-757.

HILL R., 1965, Continuum micro-mechanics of elastoplastic polycrystals, *J. Mech. Phys. Solids*, **13**, 89-101.

HULT J., TRAVNICEK L., 1983, Carrying capacity of fibre bundles with varying strength and stiffness, *J. Méc. Théor. Appl.*, **2**, 643-657.

IWAN W. D., 1967, On a class of models for the yielding behaviour of continuous and composite systems, *J. Appl. Mech.*, **34**, 612-617.

KRAJCINOVIC D., SILVA M. A. G., 1982, Statistical aspects of the continuous damage theory, *Int. J. Solids Struct.*, **18**, 551-562.

LUBARDA V. A., SUMARAC D., KRAJCINOVIC D., 1992, Hysteretic response of ductile materials subjected to cycling loads, *Recent Advances in Damage Mechanics and Plasticity*, JU J.W. Ed., 145-157, ASME Publication, AMD-Vol. 132, New York.

MASING G., 1926, Eigenspannungen und verfestigung beim messing, *Proceedings 2nd International Congress of Applied Mechanics*. Zurich.

MAYERGOYZ I. D., 1991, *Mathematical Models of Hysteresis*, Springer-Verlag, New York, 1-140.

MROZ Z., 1982, Hardening and degradation rules for metals under monotonic and cyclic loading, *J. Engng. Mater. Technol.*, **105**, 113-118.

MROZ Z., SHRIVASTAVA H. P., DUBEY R. N., 1976, A non-linear hardening model and its application to cyclic loading, *Acta Mech.*, **25**, 51-61.

PREISACH F., 1935, Über die magnetische Nachwirkung, *Z. Phys.*, **94**, 277-302.

SURESH S., 1991, *Fatigue of Materials*, Cambridge University Press, Cambridge, 77-96.

REINER M., 1958, Rheology, *Handbuch der Physik*, FLUGGE S. Ed., Springer-Verlag, Berlin.

WHITE C. S., BRONKHORST C. A., ANAND L., 1990, An improved isotropic-kinematichardening model for moderate deformation metal plasticity, *Mech. Mater.*, **10**, 127-147.

(Manuscript received February 20, 1992,
accepted February 15, 1993.)